



# Effect of aspect ratio in free-swimming plunging flexible plates



Peter Derek Yeh, Alexander Alexeev\*

George W. Woodruff School of Mechanical Engineering, Georgia Institute of Technology, Atlanta, GA 30332, USA

## ARTICLE INFO

### Article history:

Received 19 December 2014

Revised 4 May 2015

Accepted 8 July 2015

Available online 21 July 2015

### Keywords:

Lattice Boltzmann model  
Fluid-structure interaction  
Elastic swimmer

## ABSTRACT

We use three dimensional computer simulations to investigate the free swimming of plunging elastic plates with aspect ratios ranging from 0.5 to 5 in a viscous fluid with Reynolds number 250. We show that maximum velocity occurs near the first natural frequency regardless of aspect ratio, whereas the maximum swimming economy occurs away from the first natural frequency and is associated with a specific swimmer bending pattern. Moreover, we show that the low aspect ratio swimmers, those with wider spans, are not only the fastest but also the most economical. The faster speeds are associated with a decrease in effective drag for low aspect ratio plunging swimmers. We find that the recently proposed vortex-induced drag model adequately explains the drag reduction by suggesting that the smaller relative size of side vortices in low aspect ratio swimmers creates less drag per unit width.

© 2015 Elsevier Ltd. All rights reserved.

## 1. Introduction

Designing robotic underwater vehicles or flapping flyers that can imitate the motion of fish or insects using oscillating flexible appendages is an active area of research. Over the years, researchers have investigated the complex hydrodynamics of oscillating fins to understand how they can generate rapid and efficient propulsion. Early studies by Wu [1–3] and Lighthill [4–6] used two dimensional inviscid models to estimate thrust generated by oscillating filaments. These models have been recently extended to three dimensions [7]. Experiments with flexible oscillating plates [8–15], two-dimensional [16,17], and three-dimensional computational studies [18–20] have provided further insights on thrust production, cruising velocity, and efficiency in a wide parameter space. These studies indicated that fast swimming and larger thrust are related to resonance oscillations.

Since fish fins have non-rectangular geometry, several recent studies have explored the effect of shape on the swimming using undulating fins. Li, et al. [21] investigated the thrust performance of rigid three-dimensional plates with a non-rectangular geometry that represented a forked tail fin and found that forked fins are more efficient than rectangular fins. Other studies sought to optimize the fin shape using both Lighthill's theory [22,23] and viscous flow simulations with fully prescribed kinematics [24]. Each of these studies produced optimal shapes that roughly resembled a real fish – a streamlined body with a caudal fin appendage – but differ between studies. These differing outcomes and conclusions from

each study likely stem from different optimization algorithms and flow parameters. For example, Tokic and Yue [23] compared their optimal shapes to real fish and found that they are similar. On the other hand, van Rees et al. [24] found optimal shapes that differ from real fish and showed that they even outperform real fish.

While these studies provide important insights on an optimal shape for an oscillating swimmer, these inconclusive results indicate that hydrodynamic effects associated with fins of different shapes are not fully understood. Towards this goal, we systematically study the hydrodynamics of rectangular flexible fins with different aspect ratios. Specifically, we approximate the oscillating flexible fin as a thin elastic plate with a prescribed plunging motion at its leading edge. We probe the hydrodynamics of these oscillating rectangular plates, henceforth called swimmers, undergoing free swimming. In this state the swimmer experiences no net time averaged forces as thrust and drag are equally balanced, i.e. the swimmer cruises forward. We calculate the steady state swimming velocity and power consumption, quantify the swimming efficiency, and show how swimmer aspect ratio affects the swimming parameters.

## 2. Computational model

### 2.1. Geometry and system parameters

Our elastic swimmer is modeled as a thin, elastic plate with length  $L$  and width  $w$ . The plate thickness  $b$  is sufficiently small, i.e.  $b < < L$ , so the plate assumed to be infinitely thin. We characterize the swimmer geometry by the aspect ratio  $AR = L/w$ . Fig. 1 illustrates the geometry of swimmers with 3 different aspect ratios. In our simulations, we vary aspect ratio by keeping  $L$  constant and changing  $w$ . As Fig. 1 shows, the swimmer leading edge undergoes a prescribed sinusoidal

\* Corresponding author. Present address: 771 Ferst Dr., N.W., Love Bld. 215, Atlanta, GA 30332, USA. Tel.: +404 385 3659; fax: +404 894 8496.

E-mail address: [alexander.alexeev@me.gatech.edu](mailto:alexander.alexeev@me.gatech.edu) (A. Alexeev).

URL: <http://cfms.gatech.edu> (A. Alexeev)

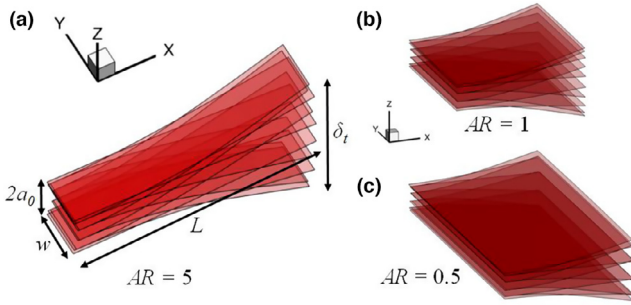


**Fig. 1.** Schematic of swimmers with aspect ratios (a)  $AR = 5$ , (b)  $AR = 1$ , and (c)  $AR = 0.5$ . In all cases, the leading edge undergoes a sinusoidal plunging motion with amplitude  $a_0$ . Overlaid are transparent snapshots of the bending pattern at different instants of time during one period when the swimmers are actuated at the natural frequency.

plunging motion given by  $a(t) = a_0 \cos(\omega t)$ , where  $a_0$  is the oscillation amplitude,  $\omega$  is the driving frequency, and  $t$  is time. Note that in our simulations we keep  $\omega$  and  $a_0$  constant.

The elastic swimmer is submerged entirely in an incompressible Newtonian fluid with viscosity  $\mu$  and density  $\rho$ . The constant driving frequency leads to a constant Reynolds number  $Re = \rho \omega a_0 L / \mu$ . In addition, the swimmer dynamic bending depends on the mass ratio between the solid and fluid,  $\chi = \rho L / \rho_s b$ , where  $\rho_s$  is the density of the solid swimmer. In this study, we fix the mass ratio to be constant and equal to 1. For wider swimmers,  $\chi$  is equivalent to the added mass of the fluid periodically displaced as the swimmer plunges through the fluid; however, for narrow swimmers the added mass can be estimated as  $\chi / AR$ .

Swimmer deformation is strongly affected by the swimmer bending rigidity  $EI$ . In any structural vibration system, the deformation response is dictated by the system's proximity to its natural frequencies (defined as the frequencies at which the system vibrates in the absence of external forces). The first natural frequency  $\omega_0$  can be found for a swimmer that is constrained to not swim forward as the frequency at which the phase between the swimmer relative deflection and root displacement is  $90^\circ$  [19]. When damping is sufficiently small, oscillations are amplified the most when the driving frequency  $\omega \approx \omega_0$ , i.e. the system is driven near its first natural frequency. In our simulations we apply a constant driving frequency, so we vary the bending rigidity to investigate the swimming near the first natural frequency. Note that the first natural frequency of the swimmer submerged in the fluid is substantially different from that in vacuum [25]. Moreover, the natural frequency in fluid depends on the plate geometry and density ratio. Therefore, we use our simulations to directly determine the bending rigidity,  $EI_0$ , that leads to the first natural frequency for the constant value of  $\omega$  used in this study. Specifically, we constrain the plunging plate from swimming forward and calculate the root and tip deflections as a function of time for different values of the bending rigidity. The bending rigidity that leads to a phase difference between relative tip deflection and root displacement of  $90^\circ$  is used as  $EI_0$ . This procedure is repeated for all aspect ratios considered in this study.

Because we keep  $\omega$  constant and vary  $EI$ , we define a quantity  $r = (EI/EI_0)^{-0.5}$  to characterize the swimmer's vibration response proximity to its first natural frequency. To first order, this quantity approximates the frequency ratio, i.e.  $r \approx \omega/\omega_0$ . Therefore, we will refer to  $r$  as the frequency ratio. Note that this parameter set allows us to keep the Reynolds number constant in our simulations while probing the effect of changing swimmer elasticity.

In our study, we focus on the effects of varying aspect ratio  $AR = L/w$  and frequency ratio  $r$ . For different aspect ratios, we expect that the geometrical changes will induce different flow patterns, thereby affecting the swimmer's propulsive capability. We as-

sess the performance of our elastic plunging swimmer by finding its dimensionless period-averaged steady state swimming velocity,  $U = \bar{U}/U_0$ , and power consumption per unit width,  $P = \bar{P}/P_0$ . Here, the dimensional quantities  $\bar{U}$  and  $\bar{P}$  are normalized by the characteristic velocity  $U_0 = \omega L / 2\pi$  and characteristic power per unit width  $P_0 = 0.5 \rho U_0^3 L$ . We also introduce the dimensionless swimming economy  $\varepsilon = U/P$ . This quantity characterizes the distance traveled per unit work. Swimmers with larger  $\varepsilon$  can travel a longer distance using the same amount of work.

## 2.2. Fluid-structure interaction model

In our fully coupled fluid-structure interaction (FSI) simulations, we use a three-dimensional lattice Boltzmann model (LBM) integrated with the lattice spring model (LSM). LBM and LSM simulate the fluid flow and plate deformation, respectively. We have previously employed this computational model to investigate the free swimming of flexible elastic plates with constant aspect ratio  $L/w = 2.5$  [19].

Briefly, LBM is a particle based mesoscale method that simulates an incompressible Newtonian fluid [26–28]. In our study we employ a D3Q19 model. In three dimensions the continuous fluid is discretized on a cubic lattice, with a set of 19 continuous velocity distribution functions,  $f_i(\mathbf{r}, \mathbf{c}_i, t)$ , characterizing the fluid at each node. Specifically,  $f_i(\mathbf{r}, \mathbf{c}_i, t)$  represents the mass density of “particles” at position  $\mathbf{r}$  and time  $t$ , propagating in direction  $i$  with velocity  $\mathbf{c}_i$ . The distribution functions evolve according to the discrete Boltzmann equation [29]. Hydrodynamic quantities are calculated as moments of  $f_i(\mathbf{r}, \mathbf{c}_i, t)$ . The fluid density is given by the sum of distribution functions,  $\rho = \sum_i f_i$ , the momentum by the first moment,  $\mathbf{j} = \sum_i \mathbf{c}_i f_i$ , and stresses by the second moment  $\Pi = \sum_i \mathbf{c}_i \mathbf{c}_i f_i$ . In our simulations we set the swimmer length  $L = 50$ , oscillation amplitude  $a_0 = 0.1L$ , fluid density  $\rho = 1$ , driving period,  $\tau = 2\pi/\omega = 2000$  and viscosity  $\mu = \pi/1000$ , which yields a fluid with Reynolds number 250. The dimensional values are given in LB units.

The solid mechanics of the elastic swimmer is simulated using LSM [19,30–33]. In LSM, the continuous, elastic solid is discretized as a network of point masses (nodes) connected by harmonic springs. As mentioned previously, the swimmer is assumed to be sufficiently thin to be modeled as a two-dimensional plate. Therefore, we model the swimmer as a triangular lattice of identical point masses connected by bending and stretching springs with stiffness  $k_s$  and  $k_b$ , respectively, as shown in Fig. 2 for the case of  $AR = 2.5$ . Here, the nodes indicate the point masses, and the straight lines connecting them depict the stretching springs. Bending springs are introduced for all straight-line triplets. The open circles indicate the nodes with prescribed kinematics at the leading edge, while the filled circles represent passive mass nodes. This particular arrangement of masses and springs simulates an elastic plate with bending rigidity  $EI = \frac{3\sqrt{3}}{4} k_b w (1 - \nu^2)$  and Poisson's ratio  $\nu = 1/3$ , determined by comparing the elastic energy density of the discretized model to that of the continuum model [34,35]. The solid nodes have equilibrium spacing  $\Delta_s = 2.325$  and

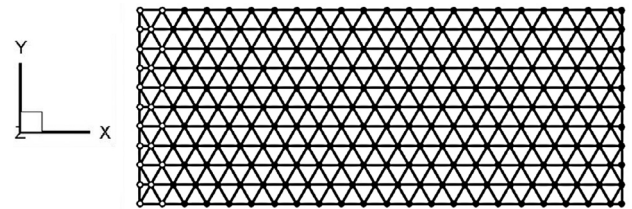


**Fig. 2.** Swimmer modeled as a triangular lattice within LSM. Open circles represent nodes with prescribed kinematics at the leading edge, while filled circles indicate positions of mass nodes. Straight lines depict stretching springs. Bending springs connect all mass node triplets on a straight line.

Download English Version:

<https://daneshyari.com/en/article/768101>

Download Persian Version:

<https://daneshyari.com/article/768101>

[Daneshyari.com](https://daneshyari.com)